J|A|C|S
ARTICLES
Published on Web 11/23/2004

Diastereoselective Alkylation of β-Amino Esters: Structural and Rate Studies Reveal Alkylations of Hexameric Lithium Enolates

Anne J. McNeil,[†] Gilman E. S. Toombes,[‡] Sol M. Gruner,[‡] Emil Lobkovsky,[†] David B. Collum,*[,†] Sithamalli V. Chandramouli,[§] Benoit J. Vanasse,[§] and Timothy A. Ayers[§]

Contribution from the Department of Chemistry and Chemical Biology, Baker Laboratory, Cornell University, Ithaca, New York 14853-1301, Physics Department, Clark Hall, Cornell University, Ithaca, New York 14853-2501, and Process Development Chemistry, Aventis, Bridgewater, New Jersey 08807

Received August 11, 2004; E-mail: dbc6@cornell.edu

Abstract: Alkylation of β-amino ester enolates proceeds with high diastereoselectivity. Single crystal, powder, and solution X-ray diffraction studies of the enolate show that the racemic enolate forms prismatic hexamers. ^{6}Li NMR spectroscopic studies on partially racemic enolates reveal complex mixtures of homo- and heterochiral hexamers. An implicit fit of the aggregate populations to the Boltzmann distribution provides the free energy differences and equilibrium constants for the ensemble. Rate studies show that enolate alkylation occurs directly from the hexamer with participation by THF. A mechanism based on the alkylation of a ladder-like aggregate is proposed.

Introduction

Otamixaban (**1**) is a small molecule, direct factor Xa inhibitor in phase IIb trials at Aventis for the management of acute coronary syndromes.[1] A key step in the preparative scale synthesis involves the enolization/alkylation sequence in eq 1.[2] The use of an unprotected amino group[3] and the resulting high diastereoselectivity (17:1) are notable. Given the prevalence of β-amino esters as components of pharmaceutical agents[4] (including β-lactam-based antibiotics),[5] we were prompted to investigate the mechanistic details of the alkylation step in the Otamixaban synthesis.

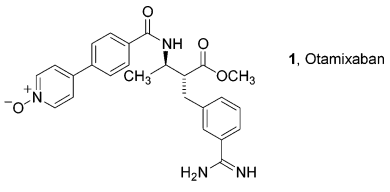

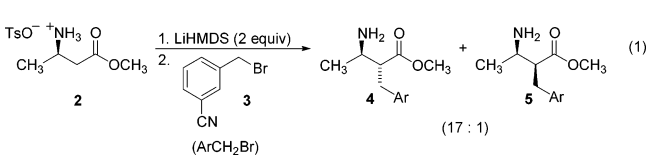

Many of the underlying structural and mechanistic questions dovetail nicely with investigations carried out at Cornell focusing on lithium hexamethyldisilazide (LiHMDS)-mediated ketone enolizations,[6] lithium diisopropylamide (LDA)-mediated ester enolizations,[7] and lithium ion solvation by protic amines.[8,9] A detailed understanding of the structures and reactivities of

[†] Department of Chemistry and Chemical Biology, Cornell University.
[‡] Physics Department, Cornell University.
[§] Aventis.

(1) Guertin, K. R.; Gardner, C. J.; Klein, S. I.; Zulli, A. L.; Czekaj, M.; Gong, Y.; Spada, A. P.; Cheney, D. L.; Maignan, S.; Guilloteau, J.-P.; Brown, K. D.; Colussi, D. J.; Chu, V.; Heran, C. L.; Morgan, S. R.; Bentley, R. G.; Dunwiddie, C. T.; Leadley, R. J.; Pauls, H. W. *Bioorg. Med. Chem. Lett.* **2002**, *12*, 1671−1674. Czekaj, M.; Klein, S. I.; Guertin, K. R.; Gardner, C. J.; Zulli, A. L.; Pauls, H. W.; Spada, A. P.; Cheney, D. L.; Brown, K. D.; Colussi, D. J.; Chu, V.; Leadley, R. J.; Dunwiddie, C. T. *Bioorg. Med. Chem. Lett.* **2002**, *12*, 1667−1670.
(2) Chandramouli, S. V.; O'Brien, M. K.; Powner, T. H. WO Patent 0040547, 2000. Nagula, G.; Huber, V. J.; Lum, C.; Goodman, B. A. *Org. Lett.* **2000**, *2*, 3527−3529.
(3) Enolates derived from unprotected α-amino amides have been alkylated: Myers, A. G.; Schnider, P.; Kwon, S.; Kung, D. W. *J. Org. Chem.* **1999**, *64*, 3322−3327. Myers, A. G.; Gleason, J. L.; Yoon, T.; Kung, D. W. *J. Am. Chem. Soc.* **1997**, *119*, 656−673. Myers, A. G.; Gleason, J. L.; Yoon, T. *J. Am. Chem. Soc.* **1995**, *117*, 8488−8489.
(4) (a) *Enantioselective Synthesis of β-Amino Acids*; Juaristi, E., Ed.; Wiley−VCH: New York, 1997. (b) For reviews: Sewald, N. *Angew. Chem. Int. Ed.* **2003**, *42*, 5794−5795. Ma, J.-A. *Angew. Chem., Int. Ed.* **2003**, *42*, 4290−4299. Liu, M.; Sibi, M. P. *Tetrahedron* **2002**, *58*, 7991−8035. Abele, S.; Seebach, D. *Eur. J. Org. Chem.* **2000**, 1−15. Cardillo, G.; Tomasini, C. *Chem. Soc. Rev.* **1996**, 117−128. Cole, D. C. *Tetrahedron* **1994**, *32*, 9517−9582. Juaristi, E.; Quintana, D.; Escalante, J. *Aldrichimica Acta* **1994**, *27*, 3−11.
(5) For leading references on the syntheses of chiral β-lactams, see: Singh, G. S. *Tetrahedron* **2003**, *59*, 7631−7649. Magriotis, P. A. *Angew. Chem. Int. Ed.* **2001**, *40*, 4377−4379. See also: *Enantioselective Synthesis of β-Amino Acids*; Juaristi, E., Ed.; Wiley−VCH: New York, 1997; pp 45−66.
(6) (a) Zhao, P.; Condo, A.; Keresztes, I.; Collum, D. B. *J. Am. Chem. Soc.* **2004**, *126*, 3113−3118. (b) Zhao, P.; Lucht, B. L.; Kenkre, S. L.; Collum, D. B. *J. Org. Chem.* **2004**, *69*, 242−249. (c) Zhao, P.; Collum, D. B. *J. Am. Chem. Soc.* **2003**, *125*, 14411−14424. (d) Zhao, P.; Collum, D. B. *J. Am. Chem. Soc.* **2003**, *125*, 4008−4009. (e) Godenschwager, P. F.; Collum, D. B., unpublished.
(7) (a) Sun, X.; Collum, D. B. *J. Am. Chem. Soc.* **2000**, *122*, 2452−2458. (b) Sun, X.; Collum, D. B. *J. Am. Chem. Soc.* **2000**, *122*, 2459−2463. (c) Sun, X.; Kenkre, S. L.; Remenar, J. F.; Gilchrist, J. H.; Collum, D. B. *J. Am. Chem. Soc.* **1997**, *119*, 4765−4766.

lithium enolates, however, has been slow to develop. Although numerous X-ray crystal structures of enolates show dimers, tetramers, and hexamers, analogous structural assignments in solution are both rare and somewhat tentative.[10,11] Colligative properties of enolate solutions shed light on the degree of aggregation[12] but can be technically challenging (especially freezing-point measurements in THF) and afford results that are quite sensitive to adventitious impurities.[13,14] NMR spectroscopy has thus far afforded limited structural details of lithium enolates. In contrast to N-lithiated and C-lithiated organolithiums, wherein $^{6}Li-^{15}N$ and $^{6}Li-^{13}C$ coupling patterns provide intimate structural details,[15] the Li−O linkages of enolates and related lithium alkoxides are spectroscopically opaque. Jackman used a combination of ^{13}C spin−lattice relaxation times and ^{7}Li quadrupole-splitting constants to show that enolates form predominantly dimers and tetramers in THF solution;[16] the accuracy and generality of this method, however, have been questioned.[17] Streitwieser used singular value decomposition of UV−vis spectra to detect monomeric, dimeric, and tetrameric phenone-derived enolates in dilute solutions.[18] Noyori exploited a combination of ^{7}Li and ^{31}P NMR spectroscopies to assign lithium cyclopentanone enolate as a dimer in HMPA/THF solutions.[17] Despite isolated successes, no general method to assign structures of lithium enolates in solution exists.

Mechanistic investigations of enolate alkylations have afforded an array of hypotheses as diverse as the enolate/solvent combinations studied. Both Jackman and Seebach suggested that enolate alkylations can proceed via tetramer-based transition structures, although the evidence is circumstantial.[19,20] Noyori recently proffered evidence for a dimer-based mechanism for the alkylation of cyclopentanone lithium enolate based on detailed rate data.[17] Streitwieser concluded that alkylations of phenone-derived lithium enolates proceed primarily via monomers.[21] To complicate the picture further, Zook, Jackman, and Streitwieser suggested that mixed aggregates derived from lithium enolates and lithium halides can alkylate directly.[22]

We describe herein studies of the alkylation of β-amino ester **6** with benzyl bromide (BnBr) shown in eq 2. Structural studies show that enolates (*R*)-**9** and *rac*-**9** exist as hexamers both in the solid state and in THF solution.[23] Rate studies reveal direct alkylations of the observable hexamers with participation by THF. Alkylations of putative hexameric ladders are discussed in the context of semiempirical computations.

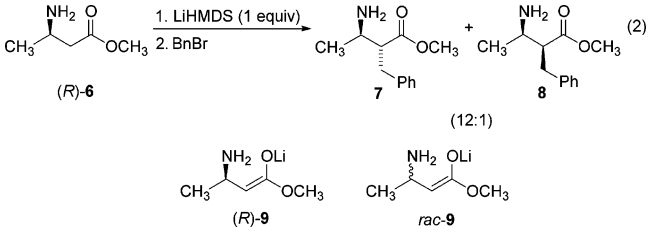

(2)

Results

Detailed spectroscopic and rate studies are described below. For brevity, most of the graphic and spectral data have been archived in the Supporting Information.

(8) (a) Aubrecht, K. B.; Lucht, B. L.; Collum, D. B. *Organometallics* **1999**, *18*, 2981−2987. (b) Lucht, B. L.; Collum, D. B. *J. Am. Chem. Soc.* **1996**, *118*, 2217−2225. (c) Lucht, B. L.; Collum, D. B. *J. Am. Chem. Soc.* **1996**, *118*, 3529−3530. (d) Also, see ref 6b.

(9) For leading references, see: Arvidsson, P. I.; Hilmersson, G.; Ahlberg, P. *J. Am. Chem. Soc.* **1999**, *121*, 1883−1887. Henderson, K. W.; Williard, P. G. *Organometallics* **1999**, *18*, 5620−5626. Vedejs, E.; Kruger, A. W.; Lee, N.; Sakata, S. T.; Stec, M.; Suna, E. *J. Am. Chem. Soc.* **2000**, *122*, 4602−4607. Laube, T.; Dunitz, J. D.; Seebach, D. *Helv. Chim. Acta* **1985**, *68*, 1373−1386.

(10) For examples of related enolate crystal structures, see: (a) Pauer, F.; Power, P. P. In *Lithium Chemistry: A Theoretical and Experimental Overview*; Sapse, A.-M., Schleyer, P. v. R., Eds.; Wiley & Sons: New York, 1995; pp 295−392. (b) Williard, P. G. *Comprehensive Organic Synthesis*; Pergamon: New York, 1991; Vol. 1, pp 1−47. (c) Seebach, D. *Angew. Chem., Int. Ed. Engl.* **1988**, *27*, 1624−1654. (d) Jastrzebski, J. T. B. H.; van Koten, G.; van de Mieroop, W. F. *Inorg. Chim. Acta* **1988**, *142*, 169−171. (e) Williard, P. G.; Tata, J. R.; Schlessinger, R. H.; Adams, A. D.; Iwanowicz, E. J. *J. Am. Chem. Soc.* **1988**, *110*, 7901−7903. (f) Seebach, D.; Amstutz, R.; Laube, T.; Schweizer, W. B.; Dunitz, J. D. *J. Am. Chem. Soc.* **1985**, *107*, 5403−5409. (g) Jastrzebski, J. T. B. H.; van Koten, G.; Christophersen, M. J. N.; Stam, C. H. *J. Organomet. Chem.* **1985**, *292*, 319−324. (h) Williard, P. G.; Carpenter, G. B. *J. Am. Chem. Soc.* **1985**, *107*, 3345−3346.

(11) For related hexameric lithium aminoalkoxide crystal structures, see: Strohmann, C.; Seibel, T.; Schildbach, D. *J. Am. Chem. Soc.* **2004**, *126*, 9876−9877. Armstrong, D. R.; Davies, R. P.; Raithby, P. R.; Snaith, R.; Wheatley, A. E. H. *New J. Chem.* **1999**, *23*, 499−507.

(12) For examples of colligative measurements on lithium enolates, see: (a) Seebach, D.; Bauer, W. *Helv. Chim. Acta* **1984**, *67*, 1972−1988. (b) Arnett, E. M.; Moe, K. D. *J. Am. Chem. Soc.* **1991**, *113*, 7288−7293. (c) Arnett, E. M.; Fisher, F. J.; Nichols, M. A.; Ribeiro, A. A. *J. Am. Chem. Soc.* **1990**, *112*, 801−808.

(13) For examples of colligative measurements on other organolithiums, see: (a) Davidson, M. G.; Snaith, R.; Stalke, D.; Wright, D. S. *J. Org. Chem.* **1993**, *58*, 2810−2816. (b) Kallman, N.; Collum, D. B. *J. Am. Chem. Soc.* **1987**, *109*, 7466−7472. (c) Wanat, R. A.; Collum, D. B.; Van Duyne, G.; Clardy, J.; DePue, R. T. *J. Am. Chem. Soc.* **1986**, *108*, 3415−3422. (d) West, P.; Waack, R. *J. Am. Chem. Soc.* **1967**, *89*, 4395−4399.

(14) Galiano-Roth, A. S.; Collum, D. B. *J. Am. Chem. Soc.* **1989**, *111*, 6772−6778. Zook, H. D.; Gumby, W. L. *J. Am. Chem. Soc.* **1960**, *82*, 1386-1389.

(15) Günther, H. *J. Braz. Chem.* **1999**, *10*, 241−262. Günther, H. In *Advanced Applications of NMR to Organometallic Chemistry*; Gielen, M., Willem, R., Wrackmeyer, B., Eds.; Wiley & Sons: New York, 1996; pp 247−290. Collum, D. B. *Acc. Chem. Res.* **1993**, *26*, 227−234.

(16) (a) Jackman, L. M.; Bortiatynski, J. *Adv. Carbanion Chem.* **1992**, *1*, 45−87. (b) Jackman, L. M.; Scarmoutzos, L. M.; DeBrosse, C. W. *J. Am. Chem. Soc.* **1987**, *109*, 5355−5361. (c) Jackman, L. M.; Szeverenyi, N. M. *J. Am. Chem. Soc.* **1977**, *99*, 4954−4962. (d) Jackman, L. M.; Lange, B. C. *Tetrahedron* **1977**, *33*, 2737−2769. (e) Jackman, L. M.; Haddon, R. C. *J. Am. Chem. Soc.* **1973**, *95*, 3687−3692. (f) This spectroscopic technique has been embraced by others, see: Wang, J. S.; Jérôme, R.; Warin, R.; Teyessié, P. *Macromolecules* **1993**, *26*, 1402−1406. Wen, J. Q.; Grutzner, J. B. *J. Org. Chem.* **1986**, *51*, 4220−4224.

(17) Suzuki, M.; Koyama, H.; Noyori, R. *Bull. Chem. Soc. Jpn.* **2004**, *77*, 259−268. Suzuki, M.; Koyama, H.; Noyori, R. *Tetrahedron* **2004**, *60*, 1571−1579.

(18) Wang, D. Z.; Kim, Y.-J.; Streitwieser, A. *J. Am. Chem. Soc.* **2000**, *122*, 10754−10760. Wang, D. Z.; Streitwieser, A. *J. Am. Chem. Soc.* **1999**, *121*, 6213−6219. Leung, S. S.-W.; Streitwieser, A. *J. Org. Chem.* **1999**, *64*, 3390−3391. Facchetti, A.; Streitwieser, A. *J. Org. Chem.* **1999**, *64*, 2281−2286. Gareyev, R.; Ciula, J. C.; Streitwieser, A. *J. Org. Chem.* **1996**, *61*, 4589−4593. Abbotto, A.; Streitwieser, A. *J. Am. Chem. Soc.* **1995**, *117*, 6358−6359.

(19) (a) Seebach, D.; Amstutz, R.; Dunitz, J. D. *Helv. Chim. Acta* **1981**, *64*, 2622−2626. (b) Jackman, L. M.; Lange, B. C. *J. Am. Chem. Soc.* **1981**, *103*, 4494−4499. Aggregate-based transition structures have been proposed for reactions of related lithium phenolates: (c) Jackman, L. M.; Chen, X. *J. Am. Chem. Soc.* **1997**, *119*, 8681−8684. (d) Jackman, L. M.; Petrei, M. M.; Smith, B. D. *J. Am. Chem. Soc.* **1991**, *113*, 3451−3458.

(20) The concept of aggregate-based reactions of enolates has been endorsed enthusiastically: (a) Streitwieser, A.; Leung, S. S.-W.; Kim, Y.-J. *Org. Lett.* **1999**, *1*, 145−147. (b) Leung, S. S.-W.; Streitwieser, A. *J. Am. Chem. Soc.* **1998**, *120*, 10557−10558. (c) Solladié-Cavallo, A.; Csaky, A. G.; Gantz, I.; Suffert, J. *J. Org. Chem.* **1994**, *59*, 5343−5346. (d) Wei, Y.; Bakthavatchalam, R. *Tetrahedron* **1993**, *49*, 2373−2390. (e) Wei, Y.; Bakthavatchalam, R.; Jin, X.-M.; Murphy, C. K.; Davis, F. A. *Tetrahedron Lett.* **1993**, *34*, 3715−3718. (f) Solladié-Cavallo, A.; Simon-Wermeister, M.-C.; Schwarz, J. *Organometallics* **1993**, *12*, 3743−3747. (g) Pospisil, P. J.; Wilson, S. R.; Jacobsen, E. N. *J. Am. Chem. Soc.* **1992**, *114*, 7585−7587. (h) Williard, P. G.; Hintze, M. J. *J. Am. Chem. Soc.* **1987**, *109*, 5539−5541. (i) Horner, J. H.; Vera, M.; Grutzner, J. B. *J. Org. Chem.* **1986**, *51*, 4212−4220. (j) Heathcock, C. H.; Lampe, J. *J. Org. Chem.* **1983**, *48*, 4330−4337. (k) House, H. O.; Gall, M.; Olmstead, H. D. *J. Org. Chem.* **1971**, *36*, 2361−2371.

(21) Wang, D. Z.; Streitwieser, A. *J. Org. Chem.* **2003**, *68*, 8936−8942. Streitwieser, A.; Kim, Y.-J.; Wang, D. Z. *Org. Lett.* **2001**, *3*, 2599−2601. Streitwieser, A.; Juaristi, E.; Kim, Y.-J.; Pugh, J. K. *Org. Lett.* **2000**, *2*, 3739−3741. Wang, D. Z.; Streitwieser, A. *Can. J. Chem.* **1999**, *77*, 654−658. Abbotto, A.; Leung, S. S.-W.; Streitwieser, A.; Kilway, K. V. *J. Am. Chem. Soc.* **1998**, *120*, 10807−10813. Abu-Hasanayn, F.; Stratakis, M.; Streitwieser, A. *J. Org. Chem.* **1995**, *60*, 4688−4689. See ref 18.

Alkylation. Sequential treatment of **2** with 2.0 equiv of LiHMDS at −20 °C followed by 1.0 equiv of 3-(bromomethyl)-benzonitrile (**3**) affords a 17:1 mixture of **4** and **5** along with 5−10% unalkylated ester. Observed byproducts include C,C- and C,N-dialkylated amino esters **10** and **11**, β-lactam **12**, and stilbene **13**. Interestingly, the C,C-dialkylated product was shown to derive primarily from the enolization and alkylation of the minor syn isomer (**5**) due to a markedly higher propensity of **5** to enolize when compared with **4** ($k_{rel} = 7$).[24] The N-alkylated product **11** derives primarily from the direct alkylation of **4** by the highly reactive electrophile during workup. β-Lactam **12** is formed from the reaction of the C-alkylated products with LiHMDS as discussed in more detail below. Stilbene **13** was shown to form by a facile reaction of **3** with Li-HMDS.[25]

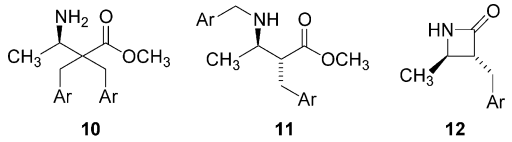

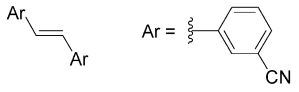

Alkylation of enolate **9** derived from either ammonium tosylate **2** or free base **6** provides similar diastereoselectivities. However, free base **6** offered considerable advantages for the structural and mechanistic studies by affording solutions of enolate **9** that were free of LiOTs.[26−29] Treatment of **6** with 1.0 equiv of LiHMDS effected the quantitative conversion of **6** (1740 cm^{-1}) to enolate **9** (1618 cm^{-1}) followed by in situ IR spectroscopy.[30] Also, we used BnBr as the electrophile instead of **3** to study the alkylation mechanism. BnBr offered attenuated rates, allowing the reaction to be conveniently monitored at 0 °C, and afforded a somewhat different reaction profile. Control experiments show that LiHMDS and BnBr do not form stilbene, and BnBr is not measurably consumed by LiHMDS. However, residual LiHMDS reacts instantaneously with **7** and **8** to afford β-lactams **14** and **15** (eq 3). In fact, alkylations using excess LiHMDS provide **14** in a preparatively useful 54% overall yield from **6** (eq 4). Finally, the alkylation shows a conversion-dependent deceleration that was traced, at least in part, to autoinhibition by LiBr.

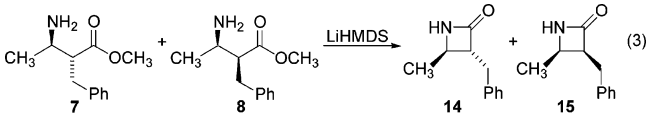

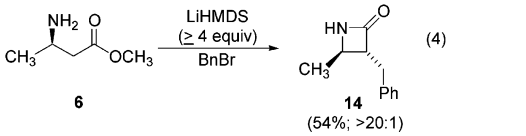

Enolate Structure: The General Problem. Determining the aggregation states of enolates in solution is particularly challenging due to the absence of Li−O coupling and the high symmetry of the most common structural forms (**16**−**19**, Chart 1). In the following sections, we present data from a number of analytical methods showing that enolate **9** is hexameric both in the solid state and in THF solution.

Chart 1

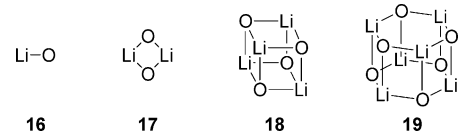

Single-Crystal X-ray Diffraction. Although we do not rely directly on X-ray crystal structures to assign aggregates in solution, X-ray studies proved critical to the development of a structural model for enolate **9**. The single-crystal X-ray structure of *rac*-**9** revealed a hexamer (Figure 1) with a drumlike core displaying S_6 symmetry.[31] The hexamer consists of three enolates of *S* configuration encircling one hexagonal face and three enolates of *R* configuration encircling the other (see **20**). The absence of coordinated THF attests to the stability of the NH_2-chelates, but we are less confident that the MeO−Li

(22) (a) Miller, J. A.; Zook, H. D. *J. Org. Chem.* **1977**, *42*, 2629−2631. (b) Jackman, L. M.; Dunne, T. S. *J. Am. Chem. Soc.* **1985**, *107*, 2805−2806. (c) Kim, Y.-J.; Streitwieser, A. *Org. Lett.* **2002**, *4*, 573−575. (d) Abu-Hasanayn, F.; Streitwieser, A. *J. Am. Chem. Soc.* **1996**, *118*, 8136−8137. (e) See ref 19b.

(23) Some of the structural studies were recently communicated: McNeil, A. J.; Toombes, G. E. S.; Chandramouli, S. V.; Vanasse, B. J.; Ayers, T. A.; O'Brien, M. K.; Lobkovsky, E.; Gruner, S. M.; Marohn, J. A.; Collum, D. B. *J. Am. Chem. Soc.* **2004**, *126*, 5938−5939.

(24) A similar selective enolization of the syn isomer was previously observed: Seebach, D.; Sifferlen, T.; Bierbaum, D. J.; Rueping, M.; Jaun, B.; Schweizer, B.; Schaefer, J.; Mehta, A. K.; O'Conner, R. D.; Meier, B. H.; Ernst, M.; Glättli, A. *Helv. Chim. Acta* **2002**, *85*, 2877−2917.

(25) LDA-mediated stilbene formation with benzyl bromide has been observed: Mali, R. S.; Jagtap, P. G. *Synth. Commun.* **1991**, *21*, 841−848.

(26) A putative LiOTs/**9** mixed aggregate forms prior to alkylation. The enolate generated from tosylate salt **2** is approximately 50% slower than the enolate generated from free base **6** in the alkylation with BnBr.

(27) For a general discussion of salt effects, see: Tchoubar, B.; Loupy, A. *Salt Effects in Organic and Organometallic Chemistry*; VCH: New York, 1992; Chapters 4, 5, and 7 and references therein.

(28) Salt effects on enolate alkylations and aldol condensations have been documented: Gutiérrez-García, V. M.; López-Ruiz, H.; Reyes-Rangel, G.; Juaristi, E. *Tetrahedron* **2001**, *57*, 6487−6496. Aurell, M. J.; Gil, S.; Mestres, R.; Parra, M.; Parra, L. *Tetrahedron* **1998**, *54*, 4357−4366. Rück, K. *Angew. Chem., Int. Ed. Engl.* **1995**, *34*, 433−435. Imai, M.; Hagihara, A.; Kawasaki, H.; Manabe, K.; Koga, K. *J. Am. Chem. Soc.* **1994**, *116*, 8829−8830. Seebach, D.; Beck, A. K.; Studer, A. In *Modern Synthetic Methods*; Ernst, B., Leumann, C., Eds.; VCH: New York, 1995; pp 1−178. Juaristi, E.; Beck, A. K.; Hansen, J.; Matt, T.; Mukhopadhyay, T.; Simson, M.; Seebach, D. *Synthesis* **1993**, 1271−1290. Bunn, B. J.; Simpkins, N. S. *J. Org. Chem.* **1993**, *58*, 533−534. Hasegawa, Y.; Kawasaki, H.; Koga, K. *Tetrahedron Lett.* **1993**, *34*, 1963−1966. Hatanaka, M.; Park, O.-S.; Ueda, I. *Tetrahedron Lett.* **1990**, *31*, 7631−7632. Murakata, M.; Nakajima, M.; Koga, K. *Chem. Commun.* **1990**, 1657−1658. Estermann, H.; Seebach, D. *Helv. Chim. Acta* **1988**, *71*, 1824−1839. Narasaka, K.; Ukaji, Y.; Watanabe, K. *Chem. Lett.* **1986**, 1755−1758. Liotta, C. L.; Caruso, T. C. *Tetrahedron Lett.* **1985**, *26*, 1599−1602. Also, see refs 10c and 22b.

(29) The role of lithium halides in the anionic polymerization of acrylates has been thoroughly examined: Dhara, M. G.; Baskaran, D.; Sivaram, S. *Macromol. Chem. Phys.* **2003**, *204*, 1567−1575. Vléek, P.; Lochmann, L. *Prog. Polym. Sci.* **1999**, *24*, 793−873. Zune, C.; Jérôme, R. *Prog. Polym. Sci.* **1999**, *24*, 631−664. Zune, C.; Dubois, P.; Jérôme, R.; Kříž, J.; Dybal, J.; Lochmann, L.; Janata, M.; Vléek, P.; Werkhoven, T. M.; Lugtenburg, J. *Macromolecules* **1998**, *31*, 2744−2755. Wang, J.-S.; Zhang, H.; Jérôme, R.; Teyssié, P. *Macromolecules* **1995**, *28*, 1758−1764. Varshney, S. K.; Gao, Z.; Zhong, X. F.; Eisenberg, A. *Macromolecules* **1994**, *27*, 1076−1082. Janata, M.; Lochmann, L.; Müller, A. H. E. *Makromol. Chem.* **1993**, *194*, 625−636. Varshney, S. K.; Hautekeer, J. P.; Fayt, R.; Jérôme, R.; Teyssié, P. *Macromolecules* **1990**, *23*, 2618−2622. Fayt, R.; Forte, R.; Jacobs, C.; Jérôme, R.; Ouhadi, T.; Teyssié, P.; Varshney, S. K. *Macromolecules* **1987**, *20*, 1442−1444.

(30) Reported pK_a values are highly solvent and substrate dependent: pK_a HMDS = 25.8 (THF): Fraser, R. R.; Mansour, T. S.; Savard, S. *J. Org. Chem.* **1985**, *50*, 3232−3234. pK_a EtOAc = 24.4 (DMSO), pK_a NH_3 = 41 (DMSO): Bordwell, F. G. *Acc. Chem. Res.* **1988**, *21*, 456−463.

(31) *rac*-**9** (0.20 M) was crystallized from a 9.0 M THF/toluene solution held at −20 °C over 24 h (CCDC 231371).

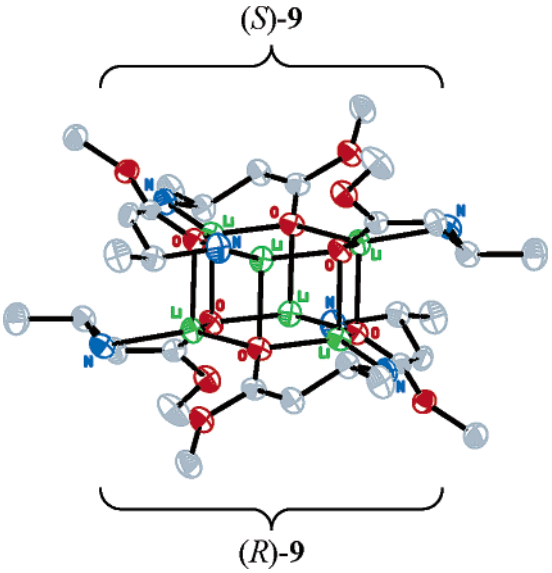

Figure 1. ORTEP of *rac*-**9** revealing a hexamer of S_6 symmetry.

interactions (Li−O = 2.6−2.8 Å) are stabilizing. Unfortunately, the highly soluble (*R*)-**9** could not be crystallized.

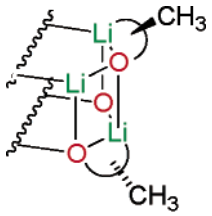

20

X-ray Powder Diffraction. We investigated whether the structure derived from a single crystal accurately described the dominant form in the bulk solid. Indeed, powder X-ray diffraction on bulk *rac*-**9** afforded a unit cell with dimensions similar to those of the crystal structure, indicating that the hexamer is the predominant solid-state aggregate of *rac*-**9**.

Small-Angle X-ray Scattering (SAXS). SAXS data on THF solutions of (*R*)-**9** or *rac*-**9** (0.5−1.5 M) showed scattering diameter and density correlations at a distance of 10 ± 4 Å. This size compares favorably with the 13 Å unit cell of the hexamer derived from *rac*-**9**. The SAXS data also confirmed the homogeneity of enolate solutions at the molarities used for the rate studies.[32]

Solution NMR Spectroscopy. We found that the inherent symmetry of the enolate aggregates described in detail above can be disrupted by using combinations of *R* and *S* antipodes to generate an ensemble of mixed aggregates.[23] What began as a problem of inordinate spectral simplicity resulting from high symmetry became a problem of extraordinary structural and spectral complexity. To understand these studies, we must briefly digress by describing dynamic phenomena that are commonly observed for organolithium aggregates but may seem surprising to the nonspecialist.

At the lowest attainable NMR probe temperatures (−100 °C), solvent exchanges,[35] conformational equilibrations,[36] and chelate isomerizations[37,38] (cf., **21**−**23**) can become slow on NMR spectroscopic time scales, often eliciting considerable spectral complexity. The spectra typically simplify on warming above −100 °C due to time averaging of these facile processes. Further warming of the probe can lead to a particularly odd effect in which intra-aggregate exchanges of ^{6}Li nuclei become fast, whereas inter-aggregate exchanges are still slow,[39] causing aggregates that differ by positional isomerism (cf., **24** and **25**) to appear as a single ^{6}Li resonance. Only aggregates that differ by subunit composition (cf., 4:2 versus 3:3 mixed hexamers **25** and **26**) or by virtue of their aggregation numbers (cf., **16**−**19**) appear as separate species by ^{6}Li NMR spectroscopy. This combination of rapid intra-aggregate exchange in conjunction with slow inter-aggregate exchange proves critical to the structural assignments of **9**.

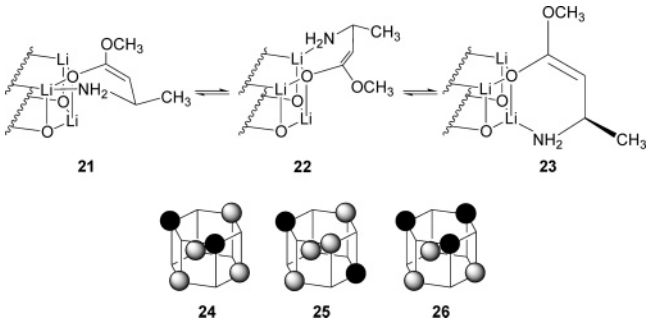

21 **22** **23**

24 **25** **26**

The ^{6}Li NMR spectrum recorded on [^{6}Li](*R*)-**9** in 9.0 M THF/toluene at −90 °C shows a single resonance (Figure 2A), consistent with almost any aggregation state of high symmetry. (The $\mathbf{R}_n\mathbf{S}_{6-n}$ notations used in Figure 2 are described below.)

(32) Follow-up studies using in situ IR spectroscopy afforded the solubility of *rac*-**9**.[33] The absorbance of solubilized *rac*-**9** during crystallization was compared with stock solutions of known molarity, showing the solubility limit to be 0.22 M in 9.0 M THF/toluene at 0 °C. In contrast, solutions of (*R*)-**9** were stable at >0.75 M in 9.0 M THF/toluene at 0 °C.[34]

(33) Attenuated total reflectance (ATR) methods allow IR spectra of liquid phases to be sampled in heterogeneous mixtures. For solubility studies using in situ IR spectroscopy, see: Fujiwara, M.; Chow, P. S.; Ma, D. L.; Braatz, R. D. *Cryst. Growth Des.* **2002**, *2*, 363−370. Togkalidou, T.; Tung, H.-H.; Sun, Y.; Andrews, A.; Braatz, R. D. *Org. Process Res. Dev.* **2002**, *6*, 317−322. Févotte, G. *Int. J. Pharm.* **2002**, *241*, 263−278. Togkalidou, T.; Fujiwara, M.; Patel, S.; Braatz, R. D. *J. Cryst. Growth* **2001**, *231*, 534−543. Dunuwila, D. D.; Berglund, K. A. *Org. Process Res. Dev.* **1997**, *1*, 350−354. Dunuwila, D. D.; Berglund, K. A. *J. Cryst. Growth* **1997**, *179*, 185−193. Dunuwila, D. D.; Carroll, L. B., II; Berglund, K. A. *J. Cryst. Growth* **1994**, *137*, 561−568.
(34) Enolates *rac*-**9** and (*R*)-**9** were shown by in situ IR spectroscopy, ^{6}Li and ^{1}H NMR spectroscopies, and GC analysis of the subsequent alkylation products to be stable in THF solutions for >2 h at 0 °C.
(35) For leading references, see: Lucht, B. L.; Collum, D. B. *Acc. Chem. Res.* **1999**, *32*, 1035−1042.
(36) Clegg, W.; Liddle, S. T.; Snaith, R.; Wheatley, A. E. H. *New J. Chem.* **1998**, *22*, 1323−1326. Boche, G.; Fraenkel, G.; Cabral, J.; Harms, K.; van Eikema Hommes, N. J. R.; Lohrenz, J.; Marsch, M.; Schleyer, P. v. R. *J. Am. Chem. Soc.* **1992**, *114*, 1562−1565. Remenar, J. F.; Lucht, B. L.; Kruglyak, D.; Romesberg, F. E.; Gilchrist, J. H.; Collum, D. B. *J. Org. Chem.* **1997**, *62*, 5748−5754.
(37) Reich, H. J.; Goldenberg, W. S.; Sanders, A. W.; Jantzi, K. L.; Tzschucke, C. C. *J. Am. Chem. Soc.* **2003**, *125*, 3509−3521 and references therein. Fraenkel, G.; Winchester, W. R. *J. Am. Chem. Soc.* **1989**, *111*, 3794−3797.
(38) For a particularly relevant description of chelate isomerization on a hexameric aggregate, see ref 8a.
(39) Arvidsson, P. I.; Ahlberg, P.; Hilmersson, G. *Chem.-Eur. J.* **1999**, *5*, 1348−1354. Bauer, W. *J. Am. Chem. Soc.* **1996**, *118*, 5450−5455. Bauer, W.; Griesinger, C. *J. Am. Chem. Soc.* **1993**, *115*, 10871−10882. DeLong, G. T.; Pannell, D. K.; Clarke, M. T.; Thomas, R. D. *J. Am. Chem. Soc.* **1993**, *115*, 7013−7014. Thomas, R. D.; Clarke, M. T.; Jensen, R. M.; Young, T. C. *Organometallics* **1986**, *5*, 1851−1857. Bates, T. F.; Clarke, M. T.; Thomas, R. D. *J. Am. Chem. Soc.* **1988**, *110*, 5109−5112. Fraenkel, G.; Hsu, H.; Su, B. M. In *Lithium: Current Applications in Science, Medicine, and Technology*; Bach, R. O., Ed.; Wiley: New York, 1985; pp 273−289. Heinzer, J.; Oth, J. F. M.; Seebach, D. *Helv. Chim. Acta* **1985**, *68*, 1848−1862. Fraenkel, G.; Henrichs, M.; Hewitt, J. M.; Su, B. M.; Geckle, M. J. *J. Am. Chem. Soc.* **1980**, *102*, 3345−3350.

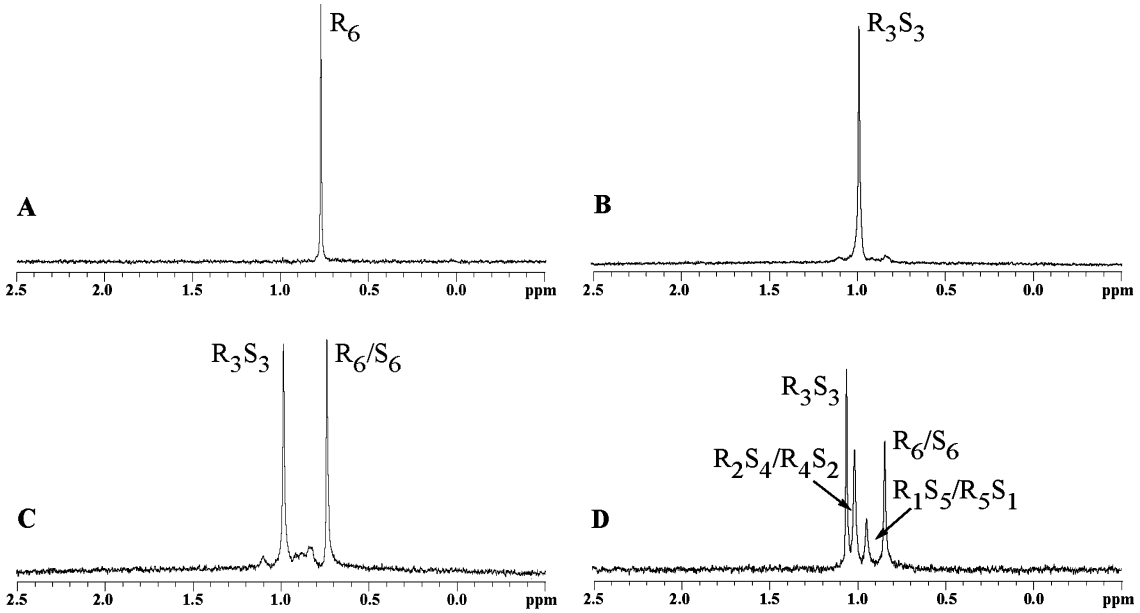

Figure 2. ^{6}Li NMR spectra in 9.0 M THF/toluene recorded on (A) [^{6}Li](*R*)-**9** (0.20 M), −90 °C; (B) [^{6}Li]*rac*-**9** (0.20 M), −90 °C; (C) [^{6}Li](*R*)-**9** (0.10 M) and [^{6}Li]*rac*-**9** (0.10 M), −90 °C; (D) [^{6}Li](*R*)-**9** (0.10 M) and [^{6}Li]*rac*-**9** (0.10 M), −50 °C.

The ^{6}Li NMR spectrum recorded on [^{6}Li]*rac*-**9** affords a single resonance at a markedly different chemical shift than [^{6}Li](*R*)-**9** (Figure 2B), suggesting the formation of a symmetric heterochiral aggregate to the exclusion of the homochiral form. Partially racemic mixtures using combinations of [^{6}Li](*R*)-**9** and [^{6}Li](*S*)-**9** at −90 °C (Figure 2C) show both resonances along with considerable "noise" in the baseline. Additionally, ^{6}Li spectra recorded on [^{6}Li,^{15}N](*R*)-**9** and [^{6}Li,^{15}N]*rac*-**9** show ^{6}Li−^{15}N coupling (d, $J_{\mathrm{Li-N}} = 3.4$ and 3.6 Hz, respectively), confirming chelation as drawn.[40,41]

Warming the probe temperature from −90 to −50 °C afforded a single sharp resonance for [^{6}Li](*R*)-**9**, which offered no evidence of latent stereoisomerism, lower symmetry, or related structural complexity. Conversely, warming samples containing varying proportions of [^{6}Li](*R*)-**9** and [^{6}Li](*S*)-**9** revealed two resonances in lieu of the baseline noise, four resonances in total (Figure 2D). The data are consistent with deep-seated structural complexities that simplify by rapid intra-aggregate exchange at elevated temperatures. Furthermore, the relative intensities are independent of the enolate (0.04−0.40 M) and the THF (2.0−9.0 M) concentrations, indicating that the four species are at the same aggregation and solvation state.

We considered models based on homochiral aggregates ($\mathbf{R}_N$ or $\mathbf{S}_N$) and heterochiral aggregates ($\mathbf{R}_n\mathbf{S}_{N-n}$). $\mathbf{R}_n\mathbf{S}_{N-n}/\mathbf{R}_{N-n}\mathbf{S}_n$ and $\mathbf{R}_N/\mathbf{S}_N$ refer to pairs of spectroscopically indistinguishable enantiomers. Dimers ($\mathbf{R_1S_1}$ and $\mathbf{R_2}/\mathbf{S_2}$) and tetramers ($\mathbf{R_4}/\mathbf{S_4}$, $\mathbf{R_1S_3}/\mathbf{R_3S_1}$, and $\mathbf{R_2S_2}$) are expected to afford two and three ^{6}Li resonances, respectively. An ensemble of homo- and heterochiral hexamers, $\mathbf{R_6}/\mathbf{S_6}$, $\mathbf{R_1S_5}/\mathbf{R_5S_1}$, $\mathbf{R_2S_4}/\mathbf{R_4S_2}$, and $\mathbf{R_3S_3}$, should afford four discrete resonances as observed. We inferred that the so-called noise in the baseline was due to positional and stereoisomerism within the $\mathbf{R_1S_5}/\mathbf{R_5S_1}$ and $\mathbf{R_2S_4}/\mathbf{R_4S_2}$ pairs in the slow exchange limit that simplified by rapid intra-aggregate exchange on warming.

A compelling picture emerges from a variant of a Job plot (Figure 3) in which the intensities of the four resonances are plotted as a function of the mole fraction of subunit (*R*)-**9**, X_R.[42] The positions of the maxima reflect the stoichiometries of the aggregates, although the relationship is more complex than that found in binary Job plots (vide infra). The concentration dependencies were modeled as follows:[43,44]

$$X_R = \frac{\sum_{n=0}^{N} n \times [R_nS_{N-n}]}{\sum_{n=0}^{N} N \times [R_nS_{N-n}]}$$

$$X_n = \frac{[R_nS_{N-n}]}{\sum_{j=0}^{N}[R_jS_{N-j}]}$$

$$[R_nS_{N-n}] = C \times \frac{N!}{n!(N-n)!} \times \phi_n \times \exp\left(\frac{n\mu_R + (N-n)\mu_S}{kT}\right)$$

where

$$\phi_n = \phi_{N-n} = \left\langle \exp\left(\frac{-g_P}{kT}\right)\right\rangle$$

X_n, the mole fraction of the aggregate, is an implicit function of X_R and ϕ_n and may be solved by an iterative parametric

(40) [^{15}N](*S*)-**6** and [^{15}N]*rac*-**6** were synthesized from [^{15}N]alanine via the Arndt−Eistert homologation: Podlech, J.; Seebach, D. *Liebigs Ann.* **1995**, 1217−1228.

(41) For calculations of ^{6}Li−^{15}N coupling constants, see: Parisel, O.; Fressigné, C.; Maddaluno, J.; Giessner-Prettre, C. *J. Org. Chem.* **2003**, *68*, 1290−1294. Koizumi, T.; Morihashi, K.; Kikuchi, O. *Bull. Chem. Soc. Jpn.* **1996**, *69*, 305−309.

(42) (a) Job, P. *Ann. Chim.* **1928**, *9*, 113−203. (b) Gil, V. M. S.; Oliveira, N. C. *J. Chem. Educ.* **1990**, *67*, 473−478.

(43) Widom, B. *Statistical Mechanics: A Concise Introduction for Chemists*; Cambridge University Press: New York, 2002.

(44) Where μ_R and μ_S are the chemical potentials of *R* and *S*, g_P corresponds to the free energy of assembly for each permutation, and *C* is a constant.

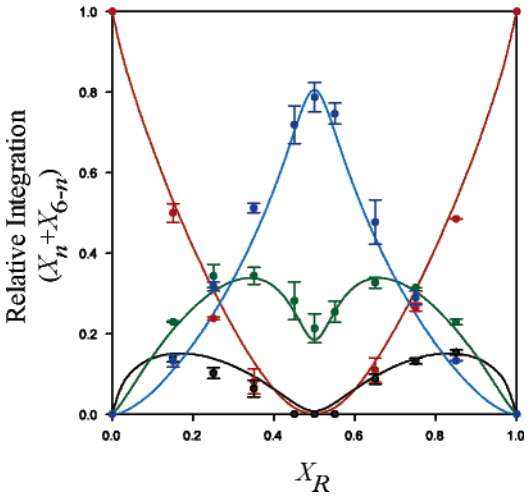

Figure 3. Job plot of the mole fraction of $\mathbf{R}_n\mathbf{S}_{6-n}/\mathbf{R}_{6-n}\mathbf{S}_n$ ($X_n + X_{6-n}$) aggregates as a function of the mole fraction of the *R* enantiomer (X_R) at −50 °C. The best fit to the data is also shown: $\mathbf{R_3S_3}$ (blue); $\mathbf{R_2S_4}/\mathbf{R_4S_2}$ (green); $\mathbf{R_1S_5}/\mathbf{R_5S_1}$ (black); $\mathbf{R_6}/\mathbf{S_6}$ (red).[45]

Table 1. Results of the Least-Squares Fits Illustrated in Figure 3

K	ΔG (kcal/mol)[a]
$K_1 = (1.0 \pm 0.1) \times 10^{-3}$	1.73 ± 0.04
$K_2 = (5.0 \pm 0.3) \times 10^{-3}$	1.82 ± 0.03
$K_3 = (115 \pm 3) \times 10^{-3}$	0.83 ± 0.01

[a] The deviations in ΔG beyond those expected for a statistical distribution were obtained from the relationship $\Delta G = -RT \ln(K/K_{statistical})$.

method. It is instructive to present the results in terms of the following equilibria:

$$\mathbf{R_3S_3} \overset{K_1}{\rightleftharpoons} {}^1/_2\mathbf{R_6} + {}^1/_2\mathbf{S_6} \qquad K_1 = \frac{\phi_0}{20\phi_3}$$

$$\mathbf{R_3S_3} \overset{K_2}{\rightleftharpoons} {}^1/_2\mathbf{R_5S_1} + {}^1/_2\mathbf{R_1S_5} \qquad K_2 = \frac{3\phi_1}{10\phi_3}$$

$$\mathbf{R_3S_3} \overset{K_3}{\rightleftharpoons} {}^1/_2\mathbf{R_4S_2} + {}^1/_2\mathbf{R_2S_4} \qquad K_3 = \frac{3\phi_2}{4\phi_3}$$

If the aggregate distribution is purely statistical ($\phi_0 = \phi_1 = \ldots = \phi_6$), then $K_1 = 0.05$, $K_2 = 0.30$, and $K_3 = 0.75$. Least-squares fits illustrated in Figure 3 yield substantially different values (Table 1). The heterochiral $\mathbf{R_3S_3}$ hexamer is markedly more stable than the alternative homo- and heterochiral combinations.

Enolate−LiX Mixed Aggregates: Solution NMR Spectroscopy. Given the possibility of mixed-aggregate intervention during the alkylation of **9**, we examined a number of **9**/LiX mixtures using ^{6}Li and ^{15}N NMR spectroscopies. Enolates (*R*)-**9** and *rac*-**9** both form mixed dimers (**27**) with excess LiHMDS.[46] The ^{6}Li NMR spectrum of a 5:1 mixture of [^{6}Li,^{15}N]LiHMDS and [^{6}Li](*R*)-**9** showed that both lithium resonances of **27** were split into a doublet (Figure 4A). The ^{6}Li NMR spectrum of a 5:1 mixture of [^{6}Li]LiHMDS and [^{6}Li,^{15}N](*S*)-**9** shows splitting of only one lithium resonance (Figure 4B). Varying the THF concentration with toluene (0.6, 3.2, 6.2, and 12.3 M) for mixtures of [^{6}Li,^{15}N]LiHMDS and [^{6}Li]*rac*-**9** or [^{6}Li](*R*)-**9** revealed that mixed dimer **27** is favored at lower THF concentrations.

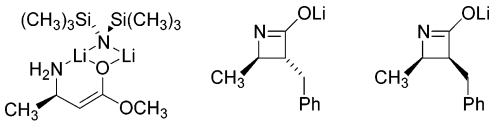

27 **28** **29**

Although excess LiHMDS influences the alkylation rates, it is not due to the formation of mixed dimer **27** per se, but rather due to the LiHMDS-mediated formation of the lithium imidates **28** and **29**, which resulted from cyclization of **7** and **8**. Spectroscopic studies of enolate **9** and imidate **28** were unsuccessful because of the marginal solubility of the lithiated lactams. The rate studies of the alkylation of **9** by BnBr suggest that LiBr generated during the course of the alkylation inhibits the reaction. Putative mixed aggregates were evidenced by the absence of an enolate homoaggregate in ^{6}Li NMR spectra recorded on [^{6}Li]**9**/[^{6}Li]LiBr mixtures, yet no detailed structural insights were available because of peak broadening.[47]

Rate Studies: General. The enolate alkylation was performed under pseudo-first-order conditions ([**9**] ≥ 10 × [BnBr]). Rates were monitored by quenching aliquots with aqueous acid, and subsequent gas chromatographic analysis measured the loss of BnBr relative to decane as an internal standard. Nonlinear least-squares fits[48] afforded the pseudo-first-order rate constants (k_{obsd}). Although rate studies of organolithium reactions often present technical hurdles that must be overcome before highly reproducible and credible data can be collected, the alkylation of **9** proved especially challenging to optimize. Some of the necessary control experiments are described below.

As noted previously, excess LiHMDS in the reaction mixture converts the alkylated β-amino esters **7** and **8** into lithiated imidates **28** and **29** with a concomitant 20% increase in the alkylation rate. Alkylations spiked with **28** displayed analogous accelerations. In addition, excess LiHMDS beyond that needed to form the lithiated imidates also marginally accelerated the enolization. Fortunately, these spurious effects could be eliminated by using a small (typically 20%) excess of β-amino ester **6** relative to LiHMDS.

Autoinhibition attributed to LiBr-derived mixed aggregates is evidenced by rate constants that are measurably (and reproducibly) different at 5% and 10% conversion (Figure 5). The effect is visible in both (*R*)-**9** and *rac*-**9** and is magnified at low THF concentrations. Exogenous LiBr added at the outset also produces the rate inhibition. This reaction may be acutely sensitive to autoinhibition because a mere 5% conversion can, at least in principle, afford enough LiBr to occlude up to 25% additional enolate in a mixed hexamer. Regardless of the origins of the conversion-dependent deceleration, the measured rate laws were indistinguishable when the rates were monitored to 5% or 10% conversion (vide infra).

Rate Laws. Plots of k_{obsd} versus [THF] for the alkylation of (*R*)-**9** and *rac*-**9** reveal approximate first-order dependencies on

(45) For the case in which $n = 3$, only X_3 is plotted (rather than $2 \times X_3$).
(46) For examples of lithium enolate−lithium amide mixed aggregates, see: Williard, P. G.; Hintze, M. J. *J. Am. Chem. Soc.* **1990**, *112*, 8602−8604. Romesberg, F. E.; Collum, D. B. *J. Am. Chem. Soc.* **1994**, *116*, 9198−9202. Hall, P. L.; Gilchrist, J. H.; Harrison, A. T.; Fuller, D. J.; Collum, D. B. *J. Am. Chem. Soc.* **1991**, *113*, 9575−9585. Also, see refs 7b, 20h, and 22c.
(47) For examples of lithium enolate−lithium halide mixed aggregates, see: (a) Henderson, K. W.; Dorigo, A. E.; Liu, Q.-Y.; Williard, P. G.; Schleyer, P. v. R.; Bernstein, P. R. *J. Am. Chem. Soc.* **1996**, *118*, 1339−1347. (b) See refs 16c, 16e, and 19b.
(48) A fit of the relative area ratios, $\text{area}_{BnBr}/\text{area}_{decane}$ (*A*), versus time to $[A] = [A]_0e^{(-kt)}$ affords the pseudo-first-order rate constants (k_{obsd}).

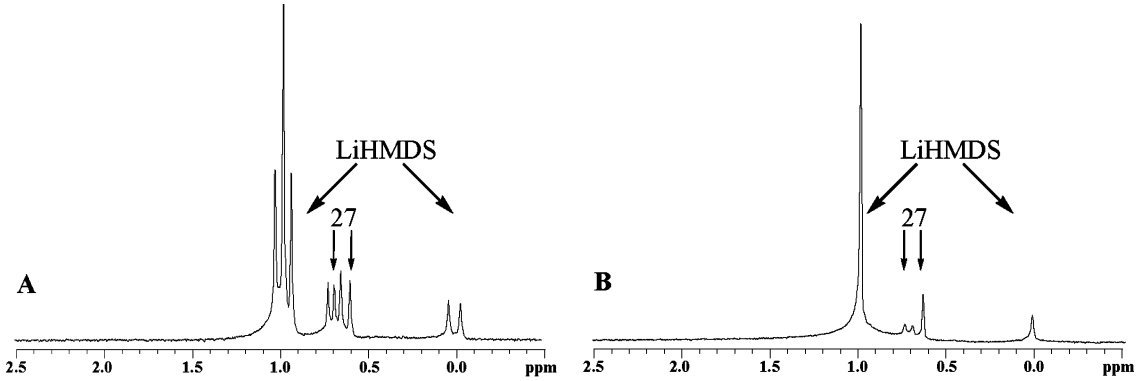

Figure 4. ^{6}Li NMR spectra in 3.1 M THF/cyclopentane recorded at −90 °C on (A) [^{6}Li,^{15}N]LiHMDS (0.14 M) and [^{6}Li](*R*)-**9** (0.03 M), δ 0.00 (d, J_{Li-N} = 4.9 Hz), 0.62 (d, J_{Li-N} = 4.0 Hz), 0.71 (d, J_{Li-N} = 2.3 Hz), 1.00 (t, J_{Li-N} = 3.7 Hz); (B) [^{6}Li]LiHMDS (0.14 M) and [^{6}Li,^{15}N](*S*)-**9** (0.03 M), δ 0.00 (s), 0.63 (s), 0.71 (d, J_{Li-N} = 3.2 Hz), 1.00 (s).

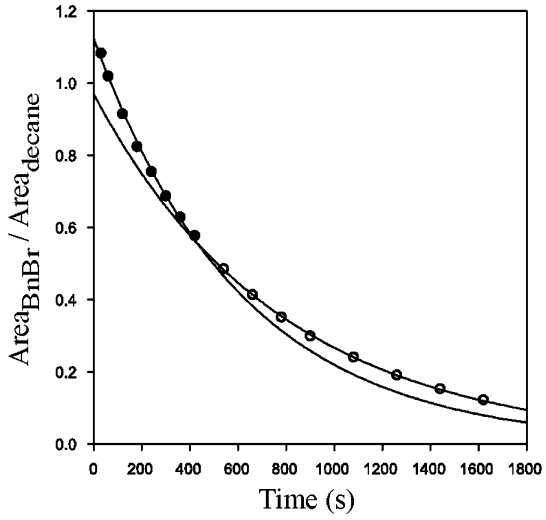

Figure 5. Relative area ratios of BnBr (area$_{BnBr}$)/decane (area$_{decane}$) versus time for the alkylation of (*R*)-**9** (0.40 M) with BnBr (0.04 M) in 3.0 M THF/toluene at 0 °C. The curves depict an unweighted least-squares fit to $[A] = [A]_o e^{(-kt)}$, where $k_{obsd} = (16.3 \pm 0.3) \times 10^{-4}$ for 0−5% conversion (●), and $k_{obsd} = (12.9 \pm 0.1) \times 10^{-4}$ for 5−10% conversion (○).

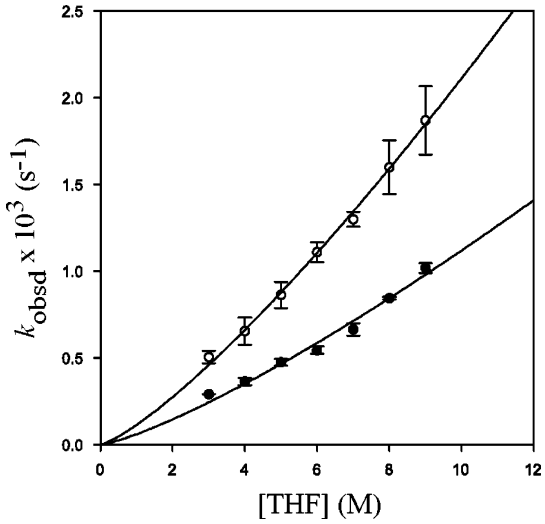

Figure 6. Plot of k_{obsd} versus [THF] with toluene for the alkylation of (*R*)-**9** (○, 0.10 M) and *rac*-**9** (●, 0.10 M), respectively, with BnBr (0.01 M) at 0 °C. The curves depict an unweighted least-squares fit to $k_{obsd} = a[\text{THF}]^n$, where $a = (1.1 \pm 0.1) \times 10^{-4}$, $n = 1.27 \pm 0.04$ for (*R*)-**9**, and $a = (6 \pm 1) \times 10^{-5}$, $n = 1.3 \pm 0.1$ for *rac*-**9**.

THF concentration ($n = 1.27 \pm 0.04$, and $n = 1.3 \pm 0.1$, respectively; Figure 6). Plots of k_{obsd} versus [(*R*)-**9**] and [*rac*-**9**] reveal approximate first-order dependencies on enolate concentration ($n = 1.05 \pm 0.04$, and $n = 0.85 \pm 0.06$, respectively; Figure 7). Despite deviations from 1.0, we are confident that the enolate orders of 0.33 or 0.16 anticipated for dimer- and monomer-based alkylations, respectively, can be excluded. The idealized rate law (eq 5)[49] implicates direct hexamer alkylation without intervening deaggregation. The approximate first orders in THF suggest the participation by one (possibly two) THF ligands.[50] The overall mechanism is depicted generically in eqs 6 and 7. Curiously, given the relative energy differences of the various $\mathbf{R}_n\mathbf{S}_{6-n}$, the rates and selectivities observed for the alkylation of **9** are surprisingly insensitive to optical purity (Table 2).

$$-\frac{\text{d[enolate]}}{\text{d}t} = k'[\text{enolate}]^1[\text{THF}]^m[\text{BnBr}]^1 \quad (5)$$

$$(\text{enolate})_6 + m\text{THF} \underset{(m=1-2)}{\rightleftharpoons} (\text{enolate})_6(\text{THF})_m \quad (6)$$

$$(\text{enolate})_6(\text{THF})_m + \text{BnBr} \rightarrow [(\text{enolate})_6(\text{THF})_m(\text{BnBr})]^{\ddagger} \rightarrow \mathbf{7} + \mathbf{8} + \text{LiBr} \quad (7)$$

Discussion

The alkylation of β-amino ester **2** used in the preparative-scale synthesis of Otamixaban (**1**) is notable due to the efficiency of using an unprotected amine. Both the importance and the residual idiosyncrasies of the protocol prompted us to investigate the underlying organolithium chemistry in greater detail. As is often the case, the mechanistic study demanded several compromises. First, it is most convenient for the preparative-scale synthesis to form the free base of ammonium tosylate **2** in situ with an additional equivalent of LiHMDS. Markedly lower alkylation rates, however, suggest that LiOTs forms mixed aggregates with the enolate.[26] Conversely, free base **6** is a superior precursor for the structural and rate studies because it affords salt-free solutions. Second, the alkylation of enolate **9** with **3** is too fast to monitor at temperatures affording homogeneous solutions,[32] so the less reactive BnBr was used to achieve tractable rates at 0 °C (eq 2). The lower reactivity of BnBr also precluded several minor side reactions, including

(49) We define the idealized rate law as that obtained by rounding the observed reaction orders to the nearest rational order.

(50) An unweighted least-squares fit of the data in Figure 6 to $k_{obsd} = a[\text{THF}]^n + b$ containing an additional adjustable parameter (*b*) affords orders in THF of 1.6 ± 0.1 and 2.2 ± 0.2 for (*R*)-**9** and *rac*-**9**, respectively.

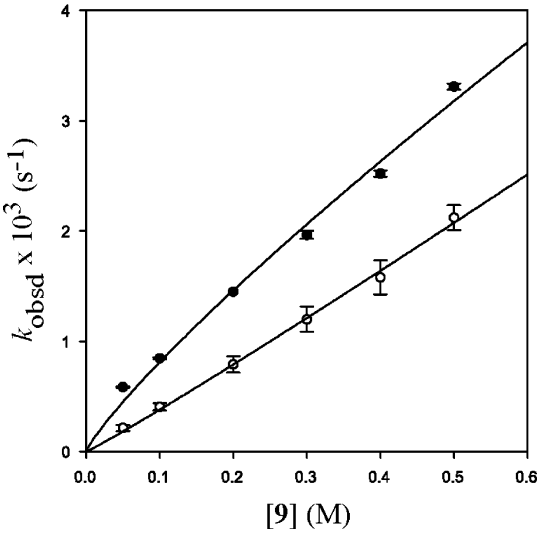

Figure 7. Plot of k_{obsd} versus [**9**] for the alkylation of (*R*)-**9** (○, 3.0 M THF/toluene) and *rac*-**9** (●, 8.0 M THF/toluene) with BnBr (0.01 M) at 0 °C. The curves depict an unweighted least-squares fit to $k_{obsd} = a[\mathbf{9}]^n$, where $a = (4.3 \pm 0.2) \times 10^{-3}$, $n = 1.05 \pm 0.04$ for (*R*)-**9**, and $a = (5.7 \pm 0.4) \times 10^{-3}$, $n = 0.85 \pm 0.06$ for *rac*-**9**.

Table 2. Relative Alkylation Rates (k_{rel}) and Diastereoselectivities (**7**:**8**) versus Optical Purity of Enolate **9**[a]

% ee	k_{rel}	**7**:**8**
0	1	12:1
50	1.5	12:1
100	1.8	13:1

[a] Reaction conditions: 9.0 M THF/toluene, 0.10 M LiHMDS, 0.12 M **6**, 0.01 M BnBr at 0 °C.

dialkylation and LiHMDS-mediated stilbene formation. By precluding stilbene formation, the LiHMDS-mediated cyclization to form β-lactams became significant (eq 3). Although the one-pot synthesis of β-lactams might be useful (eq 4), the resulting imidates **28** and **29** elicited a minor autocatalysis that proved disruptive during the rate studies. The problem was avoided by using a slight deficiency of LiHMDS for the in situ enolization.

Enolate Structure. At the outset, we confronted one of the most challenging problems in organolithium chemistry: determining the solution structures of lithium enolates. In the absence of Li−O coupling, previous investigators had turned either to specialized methods or to colligative measurements.[12,16−18] Colligative measurements offer a potentially general solution to the problem by providing solution molalities from which aggregation numbers can be inferred.[12,13] Although we had used them previously,[13b,c] it is our opinion that the high sensitivity to undetectable impurities casts significant doubts on the veracity of the method. Consequently, we explored fundamentally different strategies to study the aggregation of enolate **9**.

Standard low-temperature spectroscopic studies using ^{6}Li-labeled **9** showed that optically pure and racemic enolates, (*R*)-**9** and *rac*-**9**, each afforded spectroscopically distinct resonances consistent with homo- and heterochiral aggregates. ^{15}N-labeled enolate showed ^{6}Li−^{15}N coupling consistent with the chelates as drawn. We must confess that we believed enolate **9** was forming homo- and heterochiral dimers. However, such faith-based structural assignments have obvious limitations. In fact, the spectroscopic data were fully consistent with dimers, tetramers, hexamers, as well as any other oligomers of high symmetry (Chart 1).

A single-crystal X-ray structure and powder diffraction of *rac*-**9** revealed a hexameric aggregate containing equal proportions of (*R*)-**9** and (*S*)-**9** antipodes (denoted as $\mathbf{R_3S_3}$) to be the dominant crystalline form (Figure 1). The hexamer structure was unexpected. More to the point, crystal structures do not offer direct insights into solution structures. For example, in a recent study of lithium acetylide/lithium aminoalkoxide mixed aggregates, three species were characterized in solution, two species were characterized crystallographically, and only one form was common to both phases.[51] Curiously, the crystalline form that was observed by X-ray, but not observed in solution, was hexameric. Despite a lingering bias favoring dimers in solution, the hexamer model for the solution structure of *rac*-**9** was not easily dismissed because the structurally characterized $\mathbf{R_3S_3}$ aggregate offered a possible model to explain why *rac*-**9** forms heterochiral aggregates to the exclusion of homochiral aggregates in THF.

A break came during ^{6}Li NMR spectroscopic studies of partially racemic solutions of **9**. Along with single resonances for both *rac*-**9** and (*R*)-**9**, we observed "noise" in the baseline at −90 °C that coalesced into two new resonances (four total) on warming to −50 °C. We reasoned that the four resonances derived from an ensemble of hexamers ($\mathbf{R}_n\mathbf{S}_{6-n}$). Each aggregate could be (but is not necessarily) structurally complex due to chelate stereo and positional isomerism. The key premise was that warming the samples causes intra-aggregate exchanges, including site−site exchanges of lithium ions,[39] that would be fast on NMR spectroscopic time scales under conditions in which inter-aggregate subunit and lithium exchanges remain slow. Using the simple dimers illustratively, we would expect two ^{6}Li resonances corresponding to $\mathbf{R_2/S_2}$ and $\mathbf{R_1S_1}$. ($\mathbf{R_2}$ and $\mathbf{S_2}$ would appear as a single resonance because they are enantiomers.) In contrast, a tetramer would display three resonances corresponding to $\mathbf{R_4/S_4}$, $\mathbf{R_1S_3/R_3S_1}$, and $\mathbf{R_2S_2}$. Most important, the hexamer is predicted to afford four resonances corresponding to $\mathbf{R_6/S_6}$, $\mathbf{R_1S_5/R_5S_1}$, $\mathbf{R_2S_4/R_4S_2}$, and $\mathbf{R_3S_3}$.

The four ^{6}Li resonances are consistent with an ensemble of hexamers. Similar ensembles of hexameric *sec*-butyllithium were noted by Fraenkel.[52] Nonetheless, a more rigorous analysis was warranted. Monitoring the relative integration of the four resonances versus the mole fraction of the *R* enantiomer (optical purity) provided the results shown in Figure 3. An implicit fit to the populations using the Boltzmann distribution provides compelling support for the hexamer assignments as well as the relative energies of the aggregates. We discuss these energies further in light of the computational studies and a mechanistic hypothesis described below. It is instructive, however, to further explore implications and applications of these unusual Job plots as follows.

(1) One of the most common applications of simple Job plots in which a single mixed complex is formed (e.g., AB or AB_2) is that the position of the maximum along the *x*-axis (mole fraction) provides the stoichiometry of the complex.[42] Figure 8

(51) (a) Thompson, A.; Corley, E. G.; Huntington, M. F.; Grabowski, E. J. J.; Remenar, J. F.; Collum, D. B. *J. Am. Chem. Soc.* **1998**, *120*, 2028−2038. (b) Xu, F.; Reamer, R. A.; Tillyer, R.; Cummins, J. M.; Grabowski, E. J. J.; Reider, P. J.; Collum, D. B.; Huffman, J. C. *J. Am. Chem. Soc.* **2000**, *122*, 11212−11218.

(52) Fraenkel, G.; Henrichs, M.; Hewitt, M.; Su, B. M. *J. Am. Chem. Soc.* **1984**, *106*, 255−256.

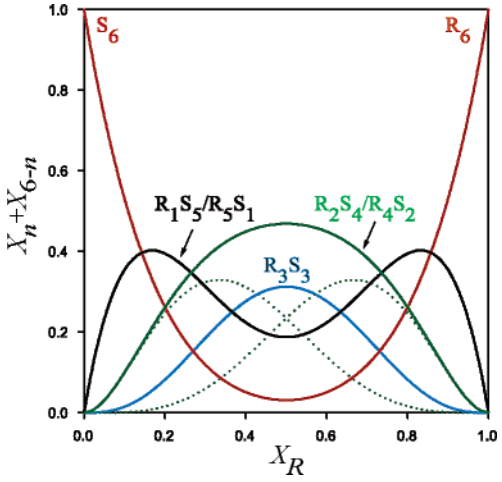

Figure 8. Job plot of the mole fraction of $\mathbf{R}_n\mathbf{S}_{6-n}/\mathbf{R}_{6-n}\mathbf{S}_n$ ($X_n + X_{6-n}$) aggregates as a function of the mole fraction of the *R* enantiomer (X_R) for the statistical case.

illustrates a plot anticipated for a purely statistical distribution of hexamers. The $\mathbf{R_3S_3}$ aggregate exhibits the anticipated maximum at $X_R = 0.5$. Although maxima would also appear for $\mathbf{R_2S_4}$ and $\mathbf{R_4S_2}$ at $X_R = 0.33$ and 0.67, respectively (dotted green curve), only one maximum is observed for the combined $\mathbf{R_2S_4/R_4S_2}$ curve (solid green curve). Furthermore, when the maxima are evident in nonstatistical cases (such as in Figure 3), their position on the *x*-axis depends on the relative energies within the ensemble. (The same holds true for the $\mathbf{R_1S_5/R_5S_1}$ curve.)

(2) An insightful referee for our preliminary communication[23] noted that an ensemble of heptamers, $\mathbf{R_7/S_7}$, $\mathbf{R_1S_6/R_6S_1}$, $\mathbf{R_2S_5/R_5S_2}$, and $\mathbf{R_3S_4/R_4S_3}$, would also afford four ^{6}Li resonances. It was tempting to dismiss this proposal on the basis of both the absence of precedence and even a structural model for such heptamers. However, it poses the more fundamental question: Can the fitting protocol rigorously distinguish two ensembles that differ in aggregation number? The short answer is that the fit of the experimental data to the heptamer model is as good as the fit to the hexamer model. This issue may become more germane in efforts to distinguish dimers ($\mathbf{R_2/S_2}$ and $\mathbf{R_1S_1}$) from trimers ($\mathbf{R_3/S_3}$ and $\mathbf{R_1S_2/R_2S_1}$), both of which *are* plausible.

(3) The strategy for determining enolate structures by monitoring an ensemble of mixed aggregates may prove generally useful. This ensemble could be achieved with pairs of antipodes via $\mathbf{R}_n\mathbf{S}_{N-n}$ mixtures or via any combination of two distinct lithium salts. For example, opposite antipodes of two different enolates, **R** and **S′**, would afford the seven hexamers of $\mathbf{R}_n\mathbf{S'}_{6-n}$, given that $\mathbf{R}_n\mathbf{S'}_{6-n}$ and $\mathbf{R}_{6-n}\mathbf{S'}_n$ would no longer be spectroscopically indistinguishable. Preliminary studies using combinations of different β-amino ester enolates support this hypothesis.

(4) Simple enolates in coordinating solvents may form tetramers rather than hexamers.[10] Therefore, we explored qualitatively what the curves would look like for an ensemble of mixed tetramers, $\mathbf{A_4}$, $\mathbf{A_3B_1}$, $\mathbf{A_2B_2}$, $\mathbf{A_1B_3}$, and $\mathbf{B_4}$. The requisite equations and the plot depicting the statistical distribution of tetramers are archived in the Supporting Information. A similar distribution of tetramers has been described.[53]

(5) We examined scenarios in which two fundamentally different aggregation states, dimers and tetramers, coexist. The

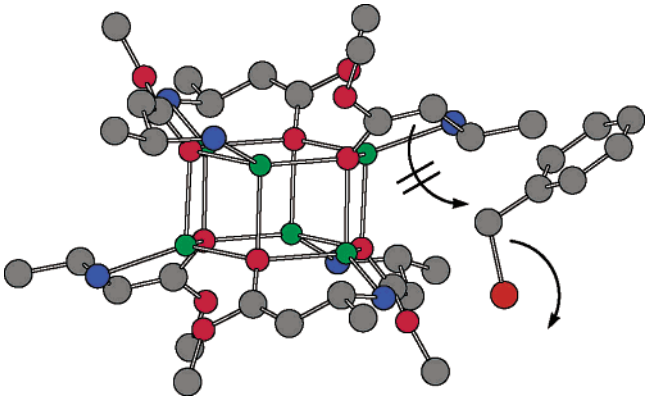

Figure 9. Anti approach of BnBr to the calculated $\mathbf{R_3S_3}$ hexamer.

results for a statistical distribution of the aggregates, $\mathbf{A_2}$, **AB**, $\mathbf{A_1B_3}$, $\mathbf{A_2B_2}$, $\mathbf{A_3B_1}$, and $\mathbf{B_4}$, and the equations for fitting experimental data can be found in the Supporting Information.

Mechanism of Alkylation. Rate studies performed under pseudo-first-order conditions revealed a first-order dependence of the rate on the enolate concentration and an approximate first-order dependence of the rate on THF concentration for both (*R*)-**9** and *rac*-**9**. In conjunction with the structural assignments, the rate studies establish the stoichiometry of the transition structures as $[(\text{enolate})_6(\text{THF})_{1-2}(\text{BnBr})]^{\ddagger}$. Although direct hexamer alkylations contrast with previous studies implicating monomer- and dimer-based mechanisms, the chelating amino group distinguishes **9** from simpler enolates.[17,21]

We considered mechanisms involving alkylation of the intact hexameric drum. Although we cannot exclude such models, they pose several problems. For example, anti approach of the benzyl bromide to the structurally characterized $\mathbf{R_3S_3}$ aggregate would be forced to occur from the congested perimeter (Figure 9). It is also difficult to imagine what role the THF would play. Consequently, we proffer an alternative mechanism based on ladders shown in eq 8. By rearranging a single chelate with the assistance of one or two THFs, the hexagonal drum can be cleaved to afford a six-rung ladder (**30**). The spirocyclic bis-chelated lithium is a known structural motif and is accessible to alkylation.[54] Although there is no direct evidence of ladder-based reactions reported to date, organolithium ladders are well documented in the structural literature largely due to the efforts of a consortium of European chemists.[55]

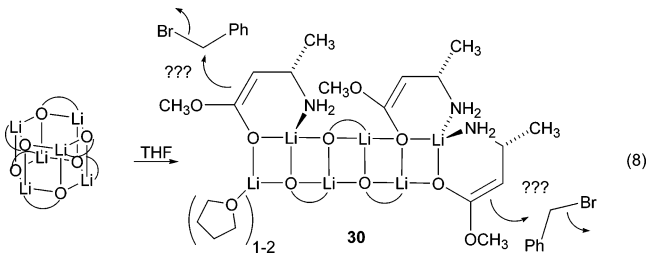

The hypothesis in eq 8 is highly speculative. Is the ladder model plausible? Does it explain the stereochemistry of alkylation? We turned to semiempirical (MNDO) computational

(53) Desjardins, S.; Flinois, K.; Oulyadi, H.; Davoust, D.; Giessner-Prettre, C.; Parisel, O.; Maddaluno, J. *Organometallics* **2003**, *22*, 4090−4097. For an application of a Job plot to identify an equilibrium mixture of titanium alkoxy and amino acid complexes, see: Weingarten, H.; Van Wazer, J. R. *J. Am. Chem. Soc.* **1965**, *87*, 724−730.

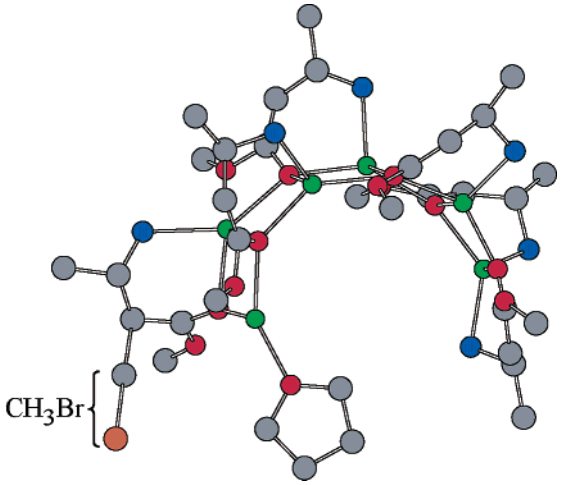

Figure 10. Transition structure for anti alkylation of the $\mathbf{R_3S_3}$ ladder with CH_3Br.

studies[56] and obtained mixed results. Minimized structures for the reactants afforded hexagonal drums exemplified by the $\mathbf{R_3S_3}$ crystal form. The calculations supported experimental evidence that the chelate orientations affording drums with S_6 ($\mathbf{R_3S_3}$) and C_3 ($\mathbf{R_6}$) symmetry are more stable than the C_3 ($\mathbf{R_3S_3}$) and D_3 ($\mathbf{R_6}$) forms (respectively). Moreover, the experimentally observed preference for the $\mathbf{R_3S_3}$ over the $\mathbf{R_6/S_6}$ form was supported. It is notable, however, that dimers $\mathbf{R_2/S_2}$ and $\mathbf{R_1S_1}$ (unsolvated) are predicted to be considerably more stable than hexamers.[57]

Preliminary investigations of the alkylation were also promising. For example, transition structures for the alkylations of the hexamer drum could not be found, whereas transition structures stemming from anti alkylation at either end of ladder **30** were viable (Figure 10).[58] Furthermore, opening the drum to an unsolvated ladder was predicted to be thermoneutral. Probing the more subtle issues pertaining to the stereochemistry of alkylation,[59] however, revealed daunting permutations arising from conformational isomerism within the chelates, the syn versus anti approach of the electrophile, the positional isomerism of the various stoichiometries, and the multiple sites available for alkylation. More to the point, the energetic differences for some of these issues appeared well within the accuracy of the computational methods.

Conclusion

Increasingly complex drug candidates demand state-of-the-art synthetic methods that are often supported by little or no mechanistic information. It is in this context that the process chemistry at Aventis and the mechanistic organolithium chemistry at Cornell find considerable synergy. The alkylation of an unprotected β-amino ester used in the preparative-scale synthesis of Otamixaban presented challenging structural and mechanistic problems. Enolates (*R*)-**9** and *rac*-**9** were characterized as an ensemble of homo- and heterochiral hexamers using a strategy based on Job plots. Although β-amino ester enolates were studied for their pharmaceutical importance, this strategy may solve the long-standing problem of characterizing enolates in solution.

The formation of enolate hexamers (rather than dimers or tetramers) was unexpected. Even more surprising, rate studies revealed that the hexamers alkylate without intervening deaggregation, suggested to proceed via ladderlike intermediates. Aggregation is often accompanied by mixed aggregation effects. Indeed, enolate **9** appeared to form mixed aggregates with a number of lithium salts causing minor autocatalysis and autoinhibition. Nonetheless, such salt effects probably influence the majority of organolithium reactions,[26−29] and the scarcity of mechanistic insights is conspicuous.[60]

Acknowledgment. We thank Prof. Cora Lind (University of Toledo) for the powder X-ray diffraction. A.J.M. and D.B.C. thank the National Institutes of Health for direct support of this work. G.E.S.T. and S.M.G. thank the DOE for support (DE-FG02-97ER62443).

Supporting Information Available: Experimental preparations, control experiments, rate data, powder X-ray diffraction data, small-angle X-ray scattering data, NMR spectroscopic data, computations, mathematical derivations, and X-ray crystallographic data (PDF, CIF). This material is available free of charge via the Internet at http://pubs.acs.org.

JA045144I

(54) Hilmersson, G.; Arvidsson, P. I.; Davidsson, O.; Håkansson, M. *J. Am. Chem. Soc.* **1998**, *120*, 8143−8149. Hilmersson, G.; Arvidsson, P. I.; Davidsson, O.; Håkansson, M. *Organometallics* **1997**, *16*, 3352−3362. Hilmersson, G.; Ahlberg, P.; Davidsson, O. *J. Am. Chem. Soc.* **1996**, *118*, 3539−3540. Veith, M. *Angew. Chem., Int. Ed. Engl.* **1987**, *26*, 1−14. See also ref 13c.

(55) For leading references to organolithium ladders, see: Mulvey, R. E. *Chem. Soc. Rev.* **1998**, *27*, 339−346. Beswick, M. A.; Wright, D. S. In *Comprehensive Organometallic Chemistry II*; Abels, E. W., Stone, F. G. A., Wilkinson, G., Eds.; Pergamon: New York, 1995; Vol. 1, Chapter 1. Gregory, K.; Schleyer, P. v. R.; Snaith, R. *Adv. Inorg. Chem.* **1991**, *37*, 47−142. Mulvey, R. E. *Chem. Soc. Rev.* **1991**, *20*, 167−209.

(56) Lithium enolates and their mixed aggregates have been examined computationally: Pratt, L. M.; Streitwieser, A. *J. Org. Chem.* **2003**, *68*, 2830−2838. Pratt, L. M.; Newman, A.; Cyr, J. S.; Johnson, H.; Miles, B.; Lattier, A.; Austin, E.; Henderson, S.; Hershey, B.; Lin, M.; Balamraju, Y.; Sammonds, L.; Cheramie, J.; Karnes, J.; Hymel, E.; Woodford, B.; Carter, C. *J. Org. Chem.* **2003**, *68*, 6387−6391. Abbotto, A.; Streitwieser, A.; Schleyer, P. v. R. *J. Am. Chem. Soc.* **1997**, *119*, 11255−11268. Weiss, H.; Yakimansky, A. V.; Müller, A. H. E. *J. Am. Chem. Soc.* **1996**, *118*, 8897−8903. Pratt, L. M.; Khan, I. M. *J. Comput. Chem.* **1995**, *16*, 1067−1080. Dybal, J.; Kříž, J. *Collect. Czech. Chem. Commun.* **1994**, *59*, 1699−1708. Romesberg, F. E.; Collum, D. B. *J. Am. Chem. Soc.* **1994**, *116*, 9187−9197. Rosi, M.; Sgamellotti, A.; Floriani, C. *J. Mol. Struct. (THEOCHEM)* **1998**, *431*, 33−46. Also, see ref 47a.

(57) Dimers $\mathbf{R_2/S_2}$ and $\mathbf{R_1S_1}$ were predicted to be 30 and 25 kcal/mol more stable than hexamers $\mathbf{R_6/S_6}$ and $\mathbf{R_3S_3}$, respectively.

(58) The absolute activation energies obtained for the ladder-based alkylation with CH_3Br were very large (∼40−43 kcal/mol). However, analogous alkylations via the monomer and the doubly chelated dimer afforded similar activation energies (∼44−51 kcal/mol).

(59) For discussions of the stereocontrol in the alkylation of lactam enolates, see: Tomoda, S.; Ikuta, Y. *Org. Lett.* **2004**, *6*, 189−192. Ikuta, Y.; Tomoda, S. *Tetrahedron Lett.* **2003**, *44*, 5931−5934. Groaning, M. D.; Meyers, A. I. *Tetrahedron* **2000**, *56*, 9843−9873. Ando, K.; Green, N. S.; Li, Y.; Houk, K. N. *J. Am. Chem. Soc.* **1999**, *121*, 5334−5335. Meyers, A. I.; Seefeld, M. A.; Lefker, B. A.; Blake, J. F.; Williard, P. G. *J. Am. Chem. Soc.* **1998**, *120*, 7429−7438. Meyers, A. I.; Seefeld, M. A.; Lefker, B. A.; Blake, J. F. *J. Am. Chem. Soc.* **1997**, *119*, 4565−4566. Seebach, D.; Maetzke, T.; Petter, W.; Klötzer, B.; Plattner, D. A. *J. Am. Chem. Soc.* **1991**, *113*, 1781−1786.

(60) For a compelling investigation of autoinhibition in the 1,2-addition of lithium acetylides to ketones, see ref 51a.